ChemComm

Accepted Manuscript

Volume 52 | Number 1 | 4 January 2016 | Pages 1–216

ChemComm

Chemical Communications
www.rsc.org/chemcomm

ISSN 1359-7345

COMMUNICATION
Marilyn M. Olmstead, Alan L. Balch, Josep M. Poblet, Luis Echegoyen et al.
Reactivity differences of Sc_NbC_{2}@n = 68 and 80: Synthesis of the first methanofullerene derivatives of Sc_NbC_{2}@C_{80}

175 YEARS

This is an Accepted Manuscript, which has been through the Royal Society of Chemistry peer review process and has been accepted for publication.

Accepted Manuscripts are published online shortly after acceptance, before technical editing, formatting and proof reading. Using this free service, authors can make their results available to the community, in citable form, before we publish the edited article. We will replace this Accepted Manuscript with the edited and formatted Advance Article as soon as it is available.

You can find more information about Accepted Manuscripts in the author guidelines.

ROYAL SOCIETY OF CHEMISTRY

rsc.li/chemcomm

Journal Name

COMMUNICATION

Intramolecular Hydrogen-Bond Activation for the Addition of Nucleophilic Imines: 2-Hydroxybenzophenone as Chemical Auxiliary[†‡]

Houcine Choubane,[a,b] Alberto F. Garrido-Castro,[a] Cuauhtemoc Alvarado,[a] Ana Martín-Somer,[c] Andrea Guerrero-Corella,[a] Mortada Daaou,[b] Sergio Díaz-Tendero,[c,d,e] Carmen Maestro,[a] Alberto Fraile,[a,e] and José Alemán*[a,e]

The addition of nucleophilic imines, using 2-hydroxybenzophenone as chemical auxiliary, is presented. An intramolecular six-membered ring via hydrogen bonding that enhances the reactivity and selectivity is the key of this strategy, which is supported by DFT calculations and experimental trials.

Wynberg published in 1981 the reaction between aromatic thiols and conjugated cycloalkenones catalysed by cinchona derivatives to afford optically active 3-arylthiocycloalkanones.[1] This paper presents a detailed investigation into the mechanism of the catalytic asymmetric system, in which a hydrogen bond between the catalyst's hydroxyl group and the enone carbonyl group, followed by deprotonation of the thiol by the quinuclidine core, is described. It therefore represents a landmark in bifunctional catalysis,[2] wherein the key role that hydrogen bonding plays in the catalytic system is highlighted. In this context, other hydrogen-bond catalysts have been developed, such as TADDOL, which has proven to be extraordinary due to the enhancement of the acidity via intramolecular activation of the hydroxyl group (OH···OH). More recently in this catalytic context, different authors, namely Takemoto,[3] Krische,[4] Vicario,[5] and Palomo[6] (top, Scheme 1), have employed different chemical auxiliaries to either increase the electrophilicity of amides or ketones, or control the stereochemistry and reactivity (nitroalkenes and aldehydes), via intramolecular hydrogen-bond activation.

In 2007, Jørgensen *et al.* described the addition of oximes to aldehydes catalysed by pyrrolidine derivatives (middle, Scheme 1).[7] Interestingly, the high electronegativity of the oxygen makes the O-H quite acid, and under the basic medium in which this reaction is performed (with 20 mol% of the Jørgensen-Hayashi catalyst), the abstraction of the proton becomes feasible, leading towards the β-addition to the iminium ion intermediate. Following derivatization, this approach gives rapid access to enantioenriched 1,3-diols. Remarkably, the obvious and analogue β-addition of an iminic nitrogen to unsaturated aldehydes, which could give access to 1,3-aminoalcohols by using the corresponding imine, has not been reported until now (middle, Scheme 1).[8] We wondered if the lack of reported work was related to the bad results yielded by the addition of these nucleophilic species, whose poor reactivity could be attributed to the low acidity of the N**H** proton compared to the O**H** proton (different electronegativity). Therefore, we considered if an intramolecular hydrogen-bond activation would facilitate the addition to the unsaturated aldehydes, providing good reactivity and enantioselectivity.

[a] Departamento de Química Orgánica (Módulo 1), Facultad de Ciencias, Universidad Autónoma de Madrid, 28049 Madrid, Spain. E-mail: jose.aleman@uam.es; webpage: www.uam.es/jose.aleman

[b] L.S.P.B.E, Département de Chimie Organique Industrielle, Faculté de Chimie, Université des Sciences et de la Technologie d'Oran- Mohamed Boudiaf- B.P 1505 El Mnaouer, Oran, 31000, Algérie.

[c] Departamento de Química (Módulo 13), Facultad de Ciencias, Universidad Autónoma de Madrid, 28049 Madrid, Spain.

[d] Condensed Matter Physics Center (IFIMAC), Universidad Autónoma de Madrid, 28049 Madrid, Spain.

[e] Institute for Advanced Research in Chemical Sciences (IAdChem), Universidad Autónoma de Madrid, 28049 Madrid, Spain.

‡ Electronic Supplementary Information (ESI) available: See DOI: 10.1039/x0xx00000x.
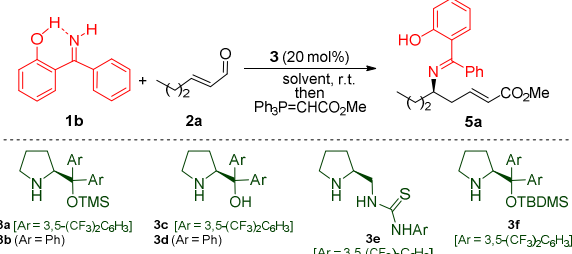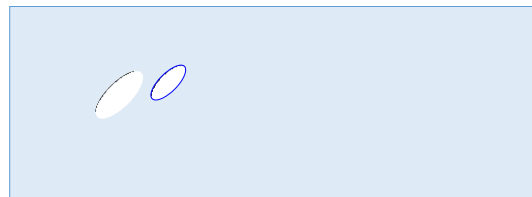
COMMUNICATION

Consequently, we looked for a chemical auxiliary that would feature the following characteristics: i) be recyclable; ii) inexpensive; and iii) removable. Considering these factors, we postulated whether 2-hydroxybenzophenone would be an appropriate candidate, since it can form a six-membered ring via intramolecular hydrogen bonding, and it can be easily released after ketimine hydrolysis. In this communication, we show how intramolecular hydrogen-bond activation is a good strategy to enhance the reactivity while also increasing the enantioselectivity. In addition, DFT calculations are included to clarify the role of the hydrogen-bond activation and to find the reasons for the noted improvements.

As a proof of concept, we performed the reaction of the commercially available **1a** with the aldehyde **2a** in the presence of catalyst **3a** at room temperature, followed by condensation to afford the Wittig product **4a** for analysis purposes (equation a, Scheme 2). Under these conditions, the reaction proceeded with low conversion (24%) and low enantioselectivity (31% *ee*) after 20h. However, when the reaction was performed with the ketimine **1b**, a dramatic change was found, noticing in this case full conversion and 80% *ee* after 20h without further optimization. With these results in hand, we began to screen the reaction (Table 1) and study the scope (Tables 2-3).

The use of different catalysts **3** has a clear influence on the final enantioselectivity (entries 1-5). Thus, sterically-hindered Jørgensen-Hayashi catalysts **3a** and **3b** were better than hydroxyl derivatives **3c** and **3d**, or thiourea catalyst **3e**. With the preliminary best catalyst in hand (**3a**), we studied different solvents such as THF, xylene and toluene, with the latter one affording the best yield and selectivity (entries 6-8). When a bulkier catalyst featuring an OTBDMS group was used (**3f**), only one enantiomer was observed. These optimal conditions (entry 9) were employed to further the scope of the aldehyde (Table 2) and nucleophile (Table 3).

The reaction tolerates different lengths in the alkyl chain, from ethyl to hexyl (entries 1-5), with very high enantioselectivities (>99%), although a slightly lower value was attained with the hexyl group (91% *ee*, entry 5). The β-isopropyl-substituted and olefin-containing α,β-unsaturated aldehydes were found to be excellent substrates for the reaction, obtaining **5f** and **5g** with complete enantioselectivities (>99%, entries 6 and 7). The inclusion of an
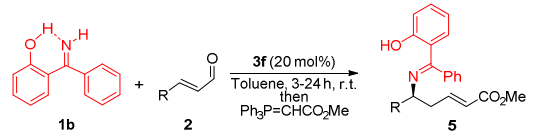
Table 1. Screening of the reaction conditions for the addition of **1b** to **2a**.[a]

Entry	Catalyst (mol%)	Solvent	Time (h)	Yield (%)[b]	*ee* (%)[c]
1	**3a** (20)	DCM	18	80	66
2	**3b** (20)	DCM	18	25	25
3	**3c** (20)	DCM	18	41	30
4	**3d** (20)	DCM	18	19	30
5	**3e** (20)	DCM	18	46	0
6	**3a** (20)	Tol	18	85	80
7	**3a** (20)	THF	18	66	80
8	**3a** (20)	Xylene	18	29	43
9	**3f (20)**	**Tol**	**6**	**70**	**>99**

[a] Reactions were performed on a 0.1 mmol scale of **1b** in 0.4 mL of the indicated solvent. [b] Isolated yields after flash chromatography. [c] Determined by chiral-SFC.

Table 2. Scope of the reaction for the addition of **1b** to different aldehydes **2**.[a]


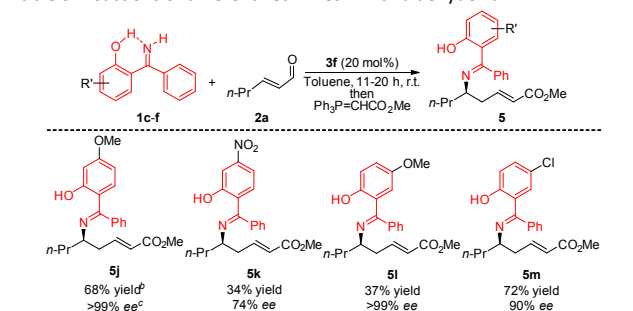| Entry	R	Yield (%)[b]	*ee* (%)[c]
1	*n*-Pr	70-**5a**	>99
2	Et	72-**5b**	>99
3	*n*-Bu	73-**5c**	>99
4	*n*-Pen	88-**5d**	>99
5	*n*-Hex	93-**5e**	91
6	*i*-Pr	85-**5f**	>99
7	CH$_2$CH$_2$CH=CH-Et	96-**5g**	>99
8	CO$_2$Et	41-**5h**	>99
9	Ph	47-**5i**	41

[a] Reactions were performed on a 0.1 mmol scale of **1b** in 0.4 mL of toluene. [b] Isolated yields after flash chromatography. [c] Determined by chiral-SFC.

ester in the β-position led to **5h** with 99% *ee* (entry 8), though diminished yield. Unfortunately, the use of an aromatic group gave **5i** with low *ee*, yet moderate yield (entry 9).

We then focused our attention on the use of different ketimines (Table 3). Different substituents at the *para* position with respect to the ketimine can be used, as shown by the successful reactions performed with ketimines **1c** (R' = MeO) and **1d** (R' = NO$_2$; with low yield and enantioselectivity). Substituents at the *para* position in relation to the hydroxyl group were also studied. Therefore, the *p*-methoxy and *p*-chloro substituted ketimines **1e** and **1f** were used, obtaining in both cases the Wittig products **5l** and **5m** with good yields and enantioselectivities. The straightforward removal of the chemical auxiliary allowed us to convert these substrates into some interesting products employing simple chemical transformations (Scheme 3). For instance, the Wittig product **5a** could be easily hydrolysed to obtain the δ-aminoester **6**
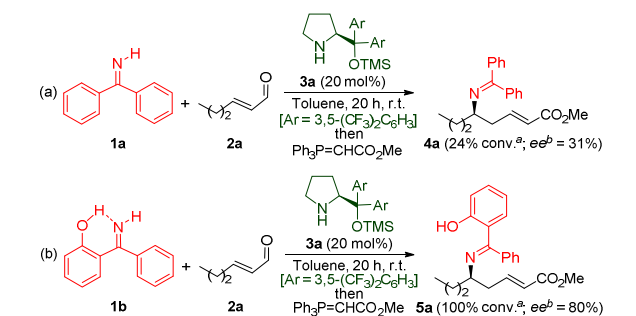
**Scheme 2.** Proof of concept in the reaction with ketimines **1a** and **1b**. [a] Determined by ^{1}H NMR. [b] Determined by chiral-SFC.

Table 3. Reactions of different ketimines **1** with aldehyde **2a**.[a]

	5j	**5k**	**5l**	**5m**
	68% yield[b]	34% yield	37% yield	72% yield
	>99% ee[c]	74% ee	>99% ee	90% ee

[a] Reactions were performed on a 0.1 mmol scale of **1** in 0.4 mL of toluene. [b] Isolated yields after flash chromatography. [c] Determined by chiral-SFC.

(equation a, Scheme 3). On the other hand, the sequential manipulations of adduct **5f** (see equation b, Scheme 3) allowed us to determine the absolute configuration of our product by chemical correlation. Firstly, complete hydrolysis of α,β-unsaturated ester **5f** gave rise to its corresponding δ-aminoacid. Then, esterification with potassium *tert*-butoxide followed by selective hydrogenation of the double bond led to δ-aminoester **7**, which has been correlated with a known (*R*)-aminoester (see ESI‡).[9] The same stereochemical outcome was assumed for the rest of compounds **5**.
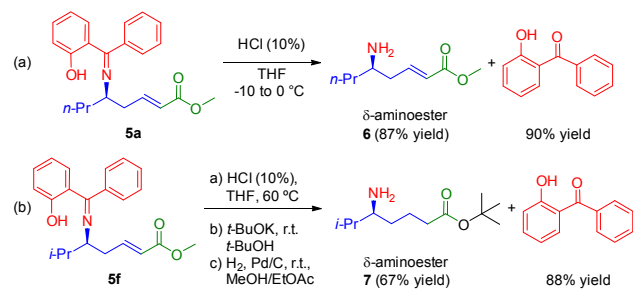
In order to obtain a complementary picture of the importance of the hydrogen-bond activation and a mechanistic approach to the reaction, we carried out Density Functional Theory simulations (SMD$_{(toluene)}$/M06-2X/6-31++G(d,p))[10] and additional experiments. We first analysed the influence of the hydroxyl group on the acidity of the ketimine, for which we considered all the possible conformations of **1a** and **1b** before and after deprotonation. The geometry for the most stable structures is shown in Figure 1, including a "Non-Covalent Interaction" analysis (NCI isosurfaces). The blue color shows the presence of hydrogen bonds while the green surfaces denote weak non-covalent interactions (for more details see the ESI‡). Ketimine **1b** displays an intramolecular hydrogen bond between the hydroxyl group and the nitrogen that is evidently absent in the **1a** derivative. As expected, this OH···NH bond makes **1b** more acidic than **1a** (by ~ 30 kcal/mol). The large increase in acidity is easily explained with the charge distribution, which was computed with a Natural Population Analysis.[11] The negative charge generated in the nitrogen atom is similar for **1a** (-0.691) and **1b** (-0.704). However, the presence of the hydroxyl group stabilizes
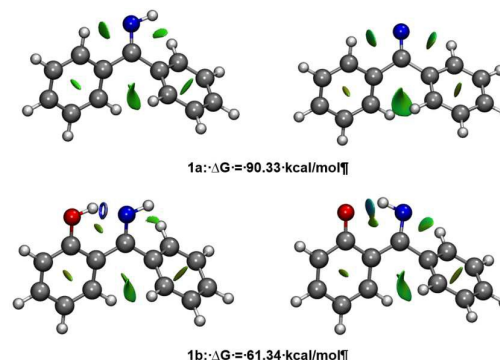
Figure 1. Gibbs free energies for deprotonated ketimine and ketimine **1a** (top), and deprotonated hydroxylketimine and hydroxylketimine **1b** (down). The gradient isosurfaces (s= 0.5 a.u.) are coloured on a BGR scale according to the sign(λ_2)ρ over the range -0.05 to 0.05 a.u.
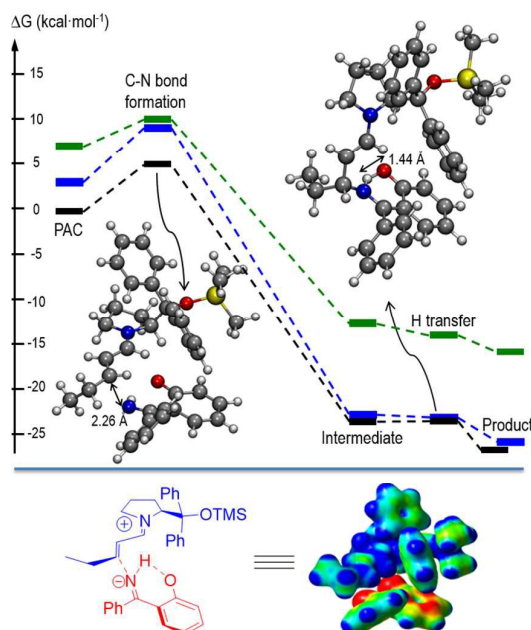
the deprotonated counterpart because: i) the more electronegative oxygen atom localizes part of the total negative charge (-0.769); and ii) the proton (+0.412) between the two negatively charged atoms stabilizes the molecule. It is interesting to note that when **1b** is deprotonated, the proton remains attached to the ketimine nitrogen. Nevertheless, a strong interaction remains between the oxygen and the proton (blue NCI surface). The rest of ketimines **1c**-**1f** show a similar behavior to **1b** (see ESI‡).

Once we determined the structure of the deprotonated ketimine, we evaluated the relative stability of the isomers in the iminium formed after condensation of aldehyde **2a** and aminocatalyst **3b**;[12] in particular, the three possible rotamers of the C-ArArOTMS group (*sc-exo*, *sc-endo* and the more stable *ap* conformation, see ESI‡).[13] Using the most stable structure for each reactant, we studied the reaction pathway (see Figure 2). Since the nucleophilic attack of the most stable ketimine to the iminium takes place from the opposite side of the bulky part of the catalyst, we considered the three possible orientations of **1b** with respect to the *ap* conformation when forming the Pre-Association Complex (PAC)[14] formed between the reactants (see ESI‡). The first and rate-limiting step consists of the formation of the C-N bond with a very low barrier of about 4 kcal/mol. This is followed by the exothermal formation of a stable intermediate, wherein the hydrogen is still covalently bonded to the nitrogen atom. In an almost concerted way, a second step with a virtually negligible barrier (~ 1 kcal/mol) takes place, involving a proton transfer to the oxygen atom, thus yielding the final addition product, which is slightly (~3 kcal/mol) more stable than the intermediate.

In a simple picture, the complete reaction undergoes a mechanism composed by a thermodynamic stage, which consists of the deprotonation of the imine formation of the PAC, followed by a kinetic step in which the new C-N bond is formed. Therefore, the thermodynamic control of the reaction is given by the acidity of the ketimine, and the kinetic control is given by the addition to the iminium. The computed mechanism indicates that the orientation of the reactants to form the PAC is crucial for the reaction to take place; in particular to the C-N bond formation. The positive charge of

(a) **5a** → δ-aminoester **6** (87% yield) + 90% yield

HCl (10%), THF, -10 to 0 °C

(b) **5f** → δ-aminoester **7** (67% yield) + 88% yield

a) HCl (10%), THF, 60 ºC
b) *t*-BuOK, r.t. *t*-BuOH
c) H$_2$, Pd/C, r.t., MeOH/EtOAc

Scheme 3. Derivatizations of ketimine products **5**.

COMMUNICATION

Journal Name

Figure 2. Gibbs free energy profile for the addition of ketimine **1b** to aldehyde **2a** catalysed by **3b**. Three different orientations for the attack of **1b** to the iminium are considered. The TSs for the C-N bond formation and H transfer in the lowest energy path are shown.

the iminium ion and the negative charge of the deprotonated ketimine suggest that the interaction between them to form the PAC must be of electrostatic nature. To understand the relative orientation of both reactants in the PAC, we computed the electrostatic potential mapped on the surface of the electron density (see bottom-right, Figure 2). The analysis of the Molecular Electrostatic Potential (MEP) shows that the attraction between the two molecules is purely electrostatic. The negative area (red) of the ketimine, localised in the nitrogen-oxygen region, interacts with the positive area of the iminium ion. The bulky part of the catalyst prevents the approach from the upper face, while in the bottom face, the cationic pocket created around the C=N bond in the iminium leads to the three possible orientations of the ketimine (green, blue and black traces, Figure 2) of the PAC considered in the computed mechanism. Only images of TSs of the kinetically most favourable pathway (black trace) have been shown for clarity (see ESI‡ for green and blue traces). To prove this hypothesis, we performed the reaction between **1b** and **2a** in the presence of tetrabutylammonium halide salts (TBAX, X = Cl, Br, I). The positive iminium ion would interact with the anionic halide. We found that the reaction
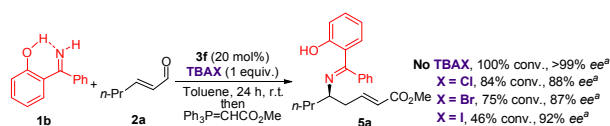
conversion decreases when the size of the halide becomes larger, which could be explained due to the large delocalization of the positive charge throughout the iminium, leading to a greater interaction with bulkier anions. This experimental result evidences the theoretical assumption of an electrostatic interaction (between the cationic chiral pocket and the anionic oxyanion of the ketimine), triggering formation of the PAC and a kinetic control exerted by the C-N bond formation once the complex is formed.

In conclusion, we have found that 2-hydroxybenzophenone is a suitable candidate to form an intramolecular six-membered ring via hydrogen bonding that can enhance the reactivity of the corresponding ketimine while also increasing the enantioselectivity in the addition to α,β-unsaturated aldehydes.

Notes and references

1 H. Hiemstra and H. Wynberg, *J. Am. Chem. Soc.* 1981, **103**, 417.
2 For selected reviews, see: (*a*) Z. Zhang and P. R. Schreiner, *Chem. Soc. Rev.* 2009, **38**, 1187; (b) J. Alemán, A. Parra, H. Jiang and K. A. Jørgensen, *Chem. Eur. J.* 2011, **17**, 6890.
3 T. Inokuma, Y. Hoashi and Y. Takemoto, *J. Am. Chem. Soc.* 2006, **128**, 9413.
4 C. K. Jung and M. J. Krische, *J. Am. Chem. Soc.* 2006, **128**, 17051.
5 G. Talavera, E. Reyes, J. L. Vicario and L. Carrillo, *Angew. Chem. Int. Ed.* 2012, **51**, 4104.
6 E. Badiola, B. Fiser, E. Gómez-Bengoa, A. Mielgo, I. Olaizola, I. Urruzuno, J. M. García, J. M. Odriozola, J. Razkin, M. Oiarbide and C. Palomo, *J. Am. Chem. Soc.* 2014, **136**, 17869.
7 S. Bertelsen, P. Dinér, R. L. Johansen, and K. A. Jørgensen, *J. Am. Chem. Soc.* 2007, **129**, 1536.
8 The 1,3-aminoalcohols can be obtained via nitrogen surrogates via iminium ion, see e.g.: For Cbz or Boc-N derivatives, see: a) Y. K. Chen, M. Yoshida and D. W. C. MacMillan, *J. Am. Chem. Soc.* 2006, **128**, 9328. b) I. Ibrahem, R. Rios, J. Vesely, G.L. Zhao and A. Córdova, *Chem. Commun*. 2007, 849. For succinamide derivatives, see c) H. Jiang, J. B. Nielsen, M. Nielsen and K. A. Jørgensen, *Chem. Eur. J.* 2007, **13**, 9068. d) I. Arenas, A. Ferrali, C. Rodríguez-Escrich, F.Bravo and M. A. Pericàs, *Adv. Synth. Catal.* 2017, **359**, 2414.
9 A. J. Burke, S. G. Davies, A. C. Garner, T. D. McCarthy, P. M. Roberts, A. D. Smith, H. Rodriguez-Solla and R. J. Vickers, *Org. Biomol. Chem.* 2004, **2**, 1387.
10 M. J. Frisch, et al. Gaussian 09, revision B.01; Gaussian, Inc.: Wallingford, CT, 2009.
11 A. E. Reed, L. A. Curtiss and F. Weinhold, *Chem. Rev*. 1988, **88**, 899.
12 We considered **3b** (with a similar reactivity as **3f**) to reduce the computational cost.
13 a) D. Seebach, U. Groselj, D. M. Badine, W. Bernd Schweizer and A. K. Beck, *Helvetica Chim. Acta,* 2008, **91**, 1999. b) Y. Hayashi, D. Okamura, T. Yamazaki, Y. Ameda, H. Gotoh, S. Tsuzuki, T. Uchimaru and D. Seebach, *Chem. Eur. J.* 2014, **20**, 17077.
14 E. M. Arpa, M. Frías, C. Alvarado, J. Alemán and S. Díaz-Tendero, *J. Mol. Catal. A: Chem.* 2016, **423**, 308.

Scheme 4. Mechanistic tests performed under the influence of TBAX. *ᵃ* Conversion determined by ¹H NMR and ee chiral-determined by SFC.

Journal Name

COMMUNICATION

GRAPHICAL ABSTRACT: